Available online at www.sciencedirect.com
ScienceDirect
Earth and Planetary Science Letters 253 (2007) 369–377
EPSL
www.elsevier.com/locate/epsl

Paleo-Moho depth determined from the pressure of CO_2 fluid inclusions: Raman spectroscopic barometry of mantle- and crust-derived rocks

Junji Yamamoto [a,*], Hiroyuki Kagi [b], Yoko Kawakami [b], Naoto Hirano [c,d], Masaki Nakamura [e]

[a] *Institute for Geothermal Sciences, Graduate School of Science, Kyoto University, Beppu 874-0903, Japan*
[b] *Geochemical laboratory, Graduate School of Science, The University of Tokyo, Hongo, Tokyo 113-0033, Japan*
[c] *Department of Earth and Planetary Sciences, Tokyo Institute of Technology, Ookayama 2-12-1, Meguro, Tokyo 152-8551, Japan*
[d] *Scripps Institution of Oceanography, University of California, San Diego, La Jolla, California, 92093-0225, USA*
[e] *Meteorological College, Asahimachi 7-4-81, Kashiwa 277-0852, Japan*

Received 8 July 2006; received in revised form 25 October 2006; accepted 27 October 2006
Available online 4 December 2006
Editor: R.W. Carlson

Abstract

The density, and therefore the pressure, of CO_2 fluid inclusions in minerals can be estimated from the Fermi diad splitting of Raman spectra of CO_2. An accurate determination of the pressure of CO_2 fluid inclusions enables the estimation of the depth origin of rocks from the deep Earth. A micro-Raman densimeter was applied to ultramafic–mafic xenoliths sampled along the Ohku coast of Oki-Dogo Island in the Sea of Japan (East Sea). The density of CO_2 fluid inclusions in the mafic granulite was 1.02–1.05 g/cm^3, while those of lherzolites were 0.98–1.02 g/cm^3. In contrast, the density of CO_2 fluid inclusions measured in olivine gabbro, clinopyroxenite, and harzburgite were lower ranging from 0.86–to 0.99 g/cm^3. Taking into account the temperature condition estimated using a pyroxene thermometer, the mafic granulite originated from a depth of 27–30 km and the lherzolites from 25–29 km. The overlapping depth of 27–29 km can be interpreted as the depth including the Moho discontinuity under Oki-Dogo Island 3.3 Ma. This estimation is consistent with geophysical observations.

Keywords: Mohorovicic discontinuity; Raman spectroscopy; fluid inclusion; CO_2; mantle xenolith; geotherm

1. Introduction

Improved knowledge of the structure of the crust and upper mantle is important for understanding their petrologic evolution and magma genesis in active island arc. The boundary between the lower crust and upper mantle, the Moho discontinuity, is determined by seismic wave velocity structures based on the considerable density gap between these two layers. Seismological observations provide very high precision estimates of the depth for the Moho discontinuity (Moho depth) in cases where sufficient seismic activity and seismic stations are available. In principle, it is possible to determine the

* Corresponding author. Fax: +81 977 22 0965.
E-mail address: jyama@bep.vgs.kyoto-u.ac.jp (J. Yamamoto).

0012-821X/$ - see front matter © 2006 Elsevier B.V. All rights reserved.
doi:10.1016/j.epsl.2006.10.038

Moho discontinuity from petrological observations by providing a depth scale for collected rock samples [1]. However, the accuracy of petrological constraints on the depth origin estimated using a geothermobarometer, e.g. that of calcium partitioning between olivine and clinopyroxene [2], is insufficient to discern the fine structure of the crust–mantle boundary. A precise barometer that is applicable to samples originating from the lower crust and upper mantle with various geologic ages can offer insight into the evolution of the global structure beneath the surface of the Earth.

A promising depth scale for rocks originating from the lower crust and upper mantle is the pressure of fluid inclusions. In general, inclusions in mantle-derived minerals retain their high internal pressure. The most prominent examples are inclusions in natural diamonds, which preserve pressures of 1–5 GPa, corresponding to the diamond stability field (>150 km) if extended to 1000 °C, a typical temperature of the upper mantle [3–8]. Silicate minerals are not as strong as diamond. Nevertheless, they can preserve the pressure in inclusions, as deduced from the fact that some CO_2 fluid inclusions in minerals appear as liquid under optical microscopic observation, even at room temperature. If the pressure, and consequently the density, of CO_2 were determined, the in-situ pressure of the trapped CO_2 could be estimated based on equilibrium temperature from a mineral thermometer when the fluid inclusions were thermally equilibrated with surrounding host minerals. The pressure is not always corresponding with the pressure of formation of the CO_2 fluid inclusions. If an upheaval of the mantle occur, the internal pressure of the CO_2 fluid inclusions in the mantle would decrease continuously by changing their volume. The internal pressure of the CO_2 fluid inclusions in mantle xenolith allows us to estimate the depth where the xenolith was entrained by host magma.

The internal pressure of CO_2 fluid inclusions can be determined using microthermometry with high precision [9–11]. However, various technical difficulties hinder the application of microthermometry to respective analyses of inclusions smaller than 5 μm, multiple component fluids, metastable states, and of inclusions comprising gas phase or low-density liquid. To overcome these difficulties, Yamamoto et al. [12] applied micro-Raman spectroscopy to the estimation of residual pressures of CO_2 fluid inclusions in mantle-derived xenoliths. Micro-Raman spectroscopy has a high spatial resolution of 1 μm and the capability of rapid analysis without encountering the inherent difficulties of microthermometry. The authors have demonstrated that mantle xenoliths from Far Eastern Russia originated from a depth up to 40 km, corresponding to the uppermost mantle. The inclusions also showed pressures that are specific to the individual host minerals, suggesting that the different densities of CO_2 fluid inclusions among the host mineral species are attributable to the minerals' rheological properties. However, accurate calibration of Raman spectra to the density (pressure) of CO_2 was not available at the time of that study — 2002. The absolute values of the CO_2 density and depth scale reported in Yamamoto et al. [12] therefore have considerable uncertain accuracy. Recently, Kawakami et al. [13] and Yamamoto and Kagi [14] measured the Raman spectra of CO_2 precisely at high pressure using a high pressure optical cell. They established a calibration between density (pressure) and Raman spectra of CO_2 over a wide range of densities: 0.1–1.24 g/cm^3. In this study, we applied spectroscopic observation of CO_2 fluid inclusions to ultramafic–mafic xenoliths from Oki-Dogo Island in the Sea of Japan and explored the depth distribution of rocks from the lower crust to the upper mantle.

2. Samples and experimental procedures

The studied samples were collected from Oki-Dogo Island, located in the southwest of the Sea of Japan, 60 km north of Honshu, Japan (Fig. 1). Mafic and ultramafic xenoliths including spinel lherzolite were obtained from a number of lava flows of alkali-olivine basalt of Oki-Dogo Island [15–18]. Basalt eruptions

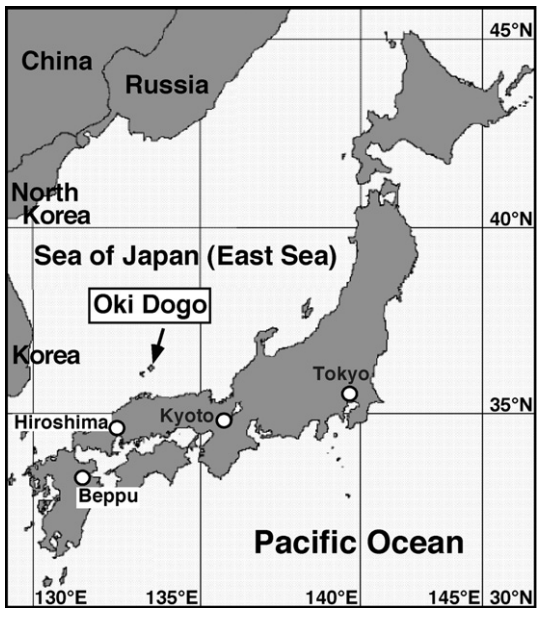

Fig. 1. Schematic map showing the location of Oki-Dogo Island.

Table 1
Average compositions (wt.%) of minerals in xenoliths from Oki Dogo

Sample	Ok5			Ok02			Ok03			Ok18	
Rock type	Harzburgite			Harzburgite			Clinopyroxenite			Olivine gabbo	
Mineral	ol	opx	cpx	ol	opx	cpx	ol	opx	cpx	ol	cpx
Mg#	81.82	83.53	84.49	82.36	83.48	83.64	84.28	83.32	82.53	76.94	83.54
Cr#											
SiO_2	39.70	54.36	51.31	40.47	54.47	51.18	42.22	54.81	51.12	38.61	50.84
TiO_2	0.01	0.20	0.98	0.03	0.34	1.14	0.04	0.40	1.55	0.01	1.19
Al_2O_3	0.02	3.84	5.88	0.21	4.64	6.52	0.03	5.55	7.88	0.01	5.11
Cr_2O_3	0.01	0.14	0.80	0.02	0.12	0.27	0.01	0.13	0.17	0.00	0.40
FeO	16.93	10.44	4.87	16.22	10.17	5.17	14.27	9.93	5.57	21.20	5.19
MnO	0.22	0.22	0.14	0.20	0.22	0.15	0.23	0.17	0.13	0.29	0.11
MgO	42.77	29.70	14.89	42.49	28.84	14.82	42.92	27.84	15.26	39.68	14.78
CaO	0.07	0.94	19.96	0.14	1.06	19.95	0.19	1.04	17.22	0.04	21.73
Na_2O	0.02	0.07	1.13	0.01	0.06	0.76	0.02	0.09	0.87	0.01	0.61
K_2O	0.02	0.02	0.02	0.02	0.03	0.02	0.02	0.02	0.02	0.01	0.03
NiO	0.22	0.08	0.0.2	0.19	0.06	0.03	0.06	0.02	0.03	0.13	0.01
P_2O_5	0.00	0.00	0.00	0.00	0.00	0.00	0.00	0.00	0.00	0.00	0.00
V_2O_3	0.00	0.00	0.00	0.00	0.00	0.00	0.00	0.00	0.00	0.00	0.00
Total	100	100	100	100	100	100	100	100	100	100	100
T [°C]	994 (34)			1038 (20)			1155 (44)				

Sample	Ok20		Ok17				Ok21			
Rock type	Mafic granulite		Lherzolite				Lherzolite			
Mineral	opx	cpx	ol	opx	cpx	sp	ol	opx	cpx	sp
Mg#	80.35	80.39	84.78	86.75	84.25	63.30	82.30	83.46	83.38	54.24
Cr#						0.14				0.24
SiO_2	52.93	49.93	40.12	54.13	52.34	0.06	40.05	54.45	51.55	0.09
TiO_2	0.26	1.00	0.00	0.21	0.78	0.43	0.01	0.28	0.86	1.16
Al_2O_3	5.88	7.88	0.02	5.12	6.43	51.39	0.02	4.00	5.70	41.33
Cr_2O_3	0.08	0.16	0.02	0.37	0.68	12.14	0.01	0.47	0.83	19.50
FeO	11.97	6.12	14.38	8.30	4.83	18.08	16.44	10.25	5.36	22.50
MnO	0.22	0.15	0.21	0.18	0.12	0.16	0.22	0.20	0.16	0.21
MgO	27.46	14.08	44.96	30.49	14.49	17.50	42.88	29.02	15.08	14.96
CaO	1.07	19.84	0.11	1.00	19.06	0.01	0.13	1.17	19.51	0.01
Na_2O	0.08	0.81	0.01	0.14	1.25	0.01	0.01	0.07	0.87	0.02
K_2O	0.02	0.02	0.02	0.02	0.02	0.02	0.01	0.01	0.02	0.02
NiO	0.03	0.02	0.15	0.04	0.02	0.20	0.20	0.07	0.05	0.20
P_2O_5	0.00	0.00	0.00	0.00	0.00	0.00	0.00	0.00	0.00	0.00
V_2O_3	0.00	0.00	0.00	0.00	0.00	0.00	0.00	0.00	0.00	0.00
Total	100	100	100	100	100	100	100	100	100	100
T [°C]	1015 (28)		1041 (29)				1048 (24)			

(ol: olivine, opx: orthopyroxene, cpx: clinopyroxene, sp: spinel).
Equilibrium temperatures (T) were estimated by two-pyroxene geothermometer of Wells [20].
Numbers in round brackets are precisions (1σ).
Major elements analyses were performed with two electron probe microanalyses (JXA8800;JEOL) at the Earthquake Research Institute, University of Tokyo and Tokyo Institute of Technology.
Analyses were carried out with an accelerating voltage of 15 kV and a beam current of 12 nA.
Multiple points in the core of a single grain of each mineral species were analyzed.

were monogenetic in every case and the K–Ar eruption ages were reported as 19–0.6 Ma [19]. We collected harzburgite, clinopyroxenite, olivine gabbro, mafic granulite, and banded spinel lherzolite samples along the Ohku coast of Oki-Dogo Island in July 2001. Major element contents of constituent minerals of the xenoliths are listed in Table 1. The present lherzolites, harzburgites and clinopyroxenite show lower Mg numbers of silicate minerals than those in typical upper mantle residual peridotites. Forsterite value [Mg/(Mg+Fe)×100] and NiO contents of the olivines deviate from the olivine–mantle array published by Takahashi [21].

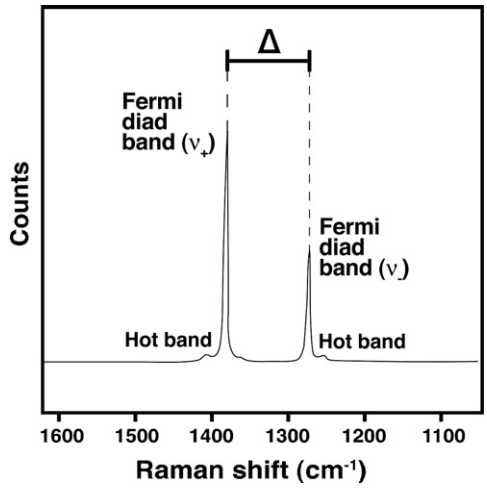

Fig. 2. Schematics of a Raman spectrum of a CO_2 fluid inclusion.

Takahashi [17] classified the xenoliths from Oki-Dogo Island into five groups in order of increasing depth: (1) mafic granulite; (2) olivine gabbro; (3) banded plagioclase peridotite; (4) banded spinel peridotite; (5) spinel lherzolite. He considered that the banded peridotite groups, including harzburgite and pyroxenite are cumulates crystallized from basaltic magma because of their microstructure and chemical compositions. The banded peridotites, however, show metamorphic deformation such as triple junctions with an angle of 120° among olivine grains. Furthermore, arrays of fluid inclusions crosscutting grain boundaries often show negative crystal, which is a form of fluid inclusion having the crystal form of host mineral, with partly spherical shape. Original cumulus textures were obliterated through subsolidus recrystallization under upper mantle conditions [18]. Therefore the Moho depth around this region corresponds to the boundary between mafic rocks (mafic granulite and olivine gabbro) and banded ultramafic rocks (banded peridotite and spinel lherzolite). The Moho depth is estimated in general using seismological methods. However, no seismic station is located nearby and the seismicity is very low in the Sea of Japan. For these reasons, we cannot presently determine the Moho depth immediately under Oki-Dogo Island precisely using seismic observations.

The samples were sliced into thin (ca. 300 μm thick) slabs, doubly polished, and mounted on a glass slide. CO_2 fluid inclusions were abundant in almost all samples. Raman spectra showed no trace of other gases such as H_2O, N_2, CH_4, etc. The CO_2 fluid inclusions studied here are almost all isolated primary inclusions consisting of pure CO_2, well away from other inclusions or healed fractures. Raman spectra of CO_2 fluid inclusions with diameters of 1–10 μm were obtained on a 30 cm single polychromator (250is; Chromex) equipped with an optical microscope (BX60; Olympus Optical Co. Ltd.), Ar ion laser (550A; Ion Laser Technology, Inc.), and a CCD camera with 1024×256 pixels (DU-401-BR-DD; Andor). The intense Rayleigh line was removed using a holographic super notch plus filter (HSPF-513.3-1.0; Kaiser Optical Systems, Inc.). An excitation laser beam with a wavelength of 514.5 nm was focused on spots of 1 or 2 μm diameter using ×100 or ×50 objectives, respectively (Olympus Optical Co. Ltd.). Laser power on the sample surface was 20 mW and the accumulation time was 5 min. The spectral resolution in the present system is approximately 1.5 cm^{-1}, but the resolution can be enhanced to 0.03 cm^{-1} by applying a curve fitting technique [13,22]. Raman spectra of CO_2 have two main peaks of v_+(1388 cm^{-1}) and v_-(1285 cm^{-1}) at ambient condition. The split (Δ) between $v_+$and v_- increases with increasing pressure (density) of CO_2. It is a reliable densimeter of CO_2 with the following relation in the density range between 0.1 and 1.24 g/cm^3: $d=-0.00111808(\Delta-100)^8+0.04498451\ (\Delta-100)^7-0.7727143(\Delta-100)^6+7.4128146\ (\Delta-100)^5-43.468301(\Delta-100)^4+159.54433\ (\Delta-100)^3-357.7651(\Delta-100)^2+448.2404\ (\Delta-100)-240.461$, where d is the density (g/cm^3) of CO_2 [14].

3. Results and discussion

3.1. Raman spectra of CO_2 fluid inclusion in the xenoliths from Oki-Dogo island

Fig. 2 depicts a typical Raman spectrum of CO_2 in fluid inclusion observed from a mantle xenolith used in this study. The splitting of the Fermi diad was estimated by applying least-squares fitting into two Lorentzian curves after subtracting a baseline from the observed spectra. Histograms of the obtained Δ values are shown in Fig. 3. The horizontal axis of Fig. 3 represents the splitting of the Fermi diad in the Raman spectra of CO_2; this variable is known to increase with increasing pressure, as indicated by the polynomial equation describing the relationship between Δ and density [13,14]. Comparisons of the depth origin of the various types of rock samples can indicate the geologic structure beneath Oki-Dogo Island and demarcate the boundary separating the crust and mantle.

3.2. Difference in residual pressure of CO_2 fluid inclusions among minerals

Before detailed comparison of depth origins of the rock samples, we will describe how to estimate the depth

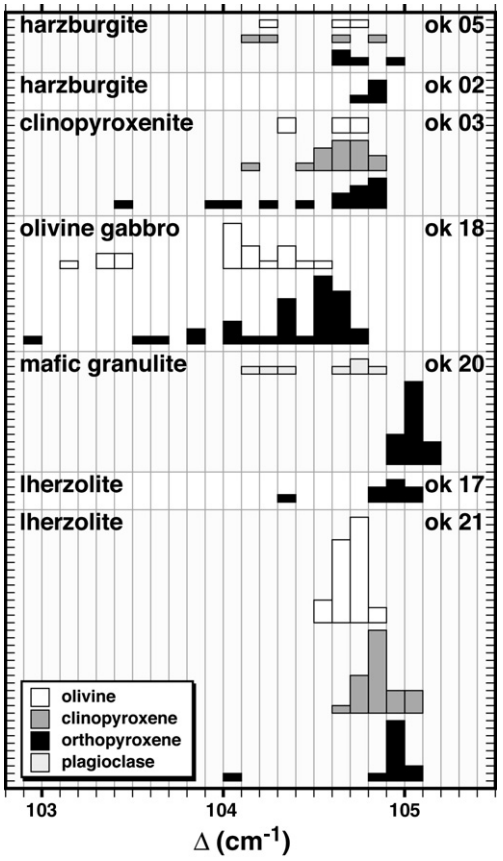

Fig. 3. Histogram of Δ values for CO_2 fluid inclusions in xenolith samples.

origin from the CO_2 density determined from Raman spectra of CO_2. The volume of the inclusion, and hence the bulk density of the CO_2, is essentially the same now as at the time of trapping because the trade-off between thermal expansion and compressibility of host mineral results in only a 2–3% volume change in elastic deformation during the ascent of mantle xenolith to the Earth's surface [12]. However, plastic deformation during ascent of mantle xenoliths might be considerable with regard to depths of the origin of mantle xenoliths. Yamamoto et al. [12] demonstrated that the residual pressures of CO_2 fluid inclusions in olivine in mantle xenoliths are systematically lower than those of orthopyroxene, clinopyroxene, or chromian spinel. Olivine underwent severe plastic deformation, thereby decreasing the residual pressure of CO_2. This mineral-specific difference in pressure suggests that the differential stress between CO_2 fluid and the surrounding olivine host mineral diminishes during ascent of the xenoliths to the Earth's surface and subsequent cooling. Results of the present study support this hypothesis because residual pressures in olivine are always lower than those in cpx and opx in the same rock sample (see Fig. 3).

In order to assess the validity of the residual pressure of CO_2 fluid inclusion as a depth probe, we simulated the density-change of the CO_2 fluid inclusions in both olivine and opx caused by plastic deformation. The density-change was calculated using a constitutive equation (Fig. 4). Fig. 4 shows the density of CO_2 fluid inclusion as a function of timescale and temperature. Differential pressure between the internal pressure of CO_2 fluid inclusion and the residual stress in the host mineral is manifested as differential stress. Under the conditions in Fig. 4, the strain rate of opx is slower than that of olivine. In the case of the CO_2 fluid inclusion in olivine having density higher than 0.6 g/cm^3, the CO_2 fluid inclusion in opx maintains initial density of 1.0 g/cm^3. In the present study, the CO_2 fluid inclusions in olivines, that show no relationship with melt inclusion, have densities higher than 0.7 g/cm^3. It is therefore appropriate to adopt the residual pressure of CO_2 fluid inclusions in opx to obtain the original depths of the rocks.

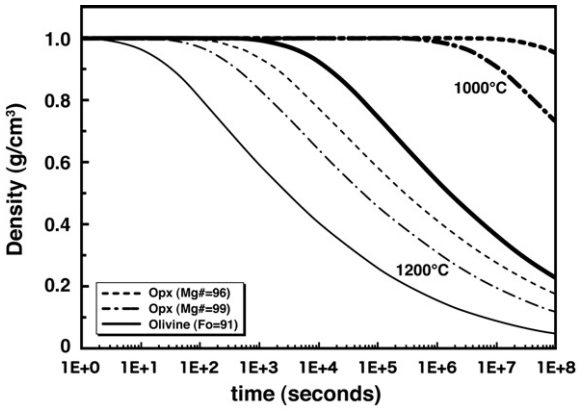

Fig. 4. Calculated change in density of CO_2 fluid inclusions in olivine and opx as a function of timescale and temperatures under oxygen fugacity (f_{O_2}) of QFM+1.5, which is restricted by the chemical equilibrium between CO and CO_2. When host basalt traps and entrains the xenoliths to near the Earth's surface, CO_2 fluid inclusions can keep pressures as high as those at the time of the trapping. Thus, the differential stress (σ) up to several hundreds of MPa would have occurred between the CO_2 fluid inclusion and surrounding crystal lattice. Then the CO_2 fluid inclusions with initial density of 1.0 g/cm^3 may expand with time. The calculation is based on constitutive equation of the diffusion creep mechanism using parameters from Bai et al. [23] for olivine and Mackwell et al. [24] for opx, respectively. The constitutive equation of single oxide mineral is expressed as:

$$\dot{e} = \dot{e}_0 f_{O_2}^m s^n \exp\left(-\frac{DH_0 + PDV}{RT}\right)$$

where $\dot{e}_0$, m, n are constants. ΔH_0, P, ΔV, R and T are activation enthalpy, hydrothermal pressure, activation volume, gas constant and temperature, respectively.

Table 2
Result of the micro-Raman spectroscopic analyses, and densities, pressures and depths calculated using the equilibrium temperatures

Sample	Rock type	Delta (cm^{-1})		Density (g/cm^3)			P (GPa)			Depth (km)		
		Median	Error	Median	Upper value	Lower value	Median	Upper value	Lower value	Median	Upper value	Lower value
Ok05	Harzburgite	104.739	0.155	0.935	0.985	0.879	0.602	0.707	0.505	21.7	25.6	18.3
Ok02	Harzburgite	104.829	0.061	0.965	0.984	0.945	0.679	0.725	0.634	24.5	26.2	22.9
Ok03	Clinopyroxenite	104.772	0.081	0.946	0.972	0.918	0.711	0.785	0.642	25.7	28.4	23.2
Ok18	Olivine gabbro	104.602	0.060	0.886	0.908	0.864						
Ok20	Mafic granulite	105.049	0.049	1.032	1.046	1.018	0.794	0.842	0.748	28.7	30.4	27.0
Ok17	Lherzolite	104.942	0.061	1.001	1.019	0.982	0.747	0.801	0.659	27.0	29.0	25.1
Ok21	Lherzolite	104.956	0.061	1.005	1.023	0.986	0.706	0.811	0.710	27.4	29.3	25.6

3.3. Estimating density of CO_2 fluid inclusion

The CO_2 fluid inclusions with lower Δ values, apart from a main cluster in the histogram (Fig. 3), were visibly decrepitated or penetrated by silicate melt inclusions. We therefore precluded those data and adopted the average of Δ values in the cluster in opx as a representative density of CO_2 fluid inclusions from Fig. 3. The Δ values for opx in mafic granulite are in the range of 105.0–105.1 cm^{-1}; those of lherzolites are in 104.9–105.0 cm^{-1} (Table 2). The Δ values of harzburgites, clinopyroxenite and olivine gabbro are considerably lower than those of mafic granulite and lherzolites. This density contrast suggests that harzburgites, clinopyroxenite and olivine gabbro originated from shallower depths than mafic granulite and lherzolites at this sample location.

Another noteworthy point is the difference in the mineral-specific contrasts of Δ values between Oki-Dogo Island and Far Eastern Russia. The difference in Δ values between cpx/opx and olivine for Far Eastern Russia reported by Yamamoto et al. [12] is approximately 0.5 cm^{-1}. In contrast, the difference for Oki-Dogo Island is up to 0.3 cm^{-1} and Δ values mutually overlap (see Fig. 3). This contrast suggests that mantle xenoliths from Far Eastern Russia underwent more severe strain than those from Oki-Dogo Island studied here. The difference in Δ values between the two mineral species may be an indicator of strain which reflects plastic deformation rate, cooling rate, eruption rate, etc. Further detailed study will be necessary to advance a more quantitative treatment of this aspect.

3.4. Depth provenance of xenoliths

The relationship between Δ value and density of CO_2 established by Yamamoto and Kagi [14] allows estimation of the densities of CO_2 fluid inclusion: 1.02–1.05 g/cm^3 and 0.98–1.02 g/cm^3 for mafic granulite and lherzolites, respectively. To estimate the pressure condition of CO_2 fluid inclusions in cases where the xenoliths were trapped by host magma, the temperature condition must be raised to that of the mantle. The equilibrium temperatures of the present samples were determined from the chemical compositions of coexisting pyroxenes. The equilibrium temperatures of lherzolites estimated from the pyroxene thermometer of Wells [20] are 1041±29 and 1048±24 °C for ok17 and ok21, respectively. The equilibrium temperature of mafic granulite is 1015±28°C. The pressure of CO_2 at a given density and temperature can be estimated (see Table 2 and Fig. 5) from the P–T diagram of CO_2 [25]. The respective pressures estimated from the density of CO_2 are 0.75–0.84 GPa and 0.70–0.81 GPa for mafic granulite and lherzolites. These pressures reflect the environment in which trapped CO_2

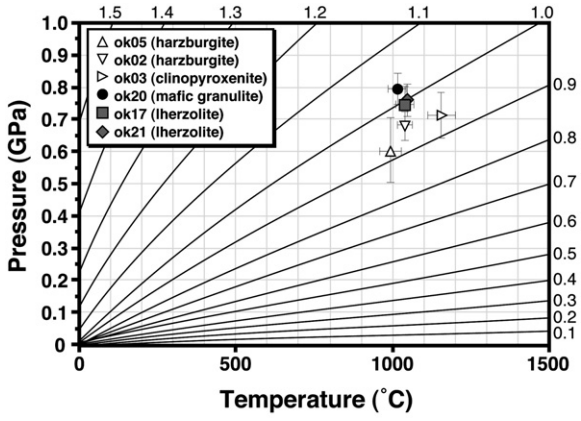

Fig. 5. P–T diagram for the system CO_2, from Pitzer and Sterner [25]. Contours represent density in g/cm^3 (i.e. isochores). Fluid inclusion pressure can be estimated from the density of CO_2 fluid inclusions and the temperature obtained using the pyroxene thermometer [20].

fluid was lithostatically equilibrated with surrounding host minerals.

Assuming the density of the crust at Oki-Dogo Island is 2.85 g/cm^3, the depth for mafic granulite was in the range of 27–30 km and that for lherzolites were 25–29 km. These estimates include some ambiguity resulting from the rock density. Mafic granulite is expected to originate from the lower crust and lherzolites from the upper mantle; the boundary between these rocks corresponds to the Moho discontinuity. The present results show that the rocks studied here coincidentally originated from almost equal depths. We can therefore determine the Moho depth under Oki-Dogo Island as 27–29 km from the overlap between mafic granulite and lherzolite.

The pressures estimated for harzburgites and clinopyroxenite are comparatively low. Major element compositions and metarmorphic deformation structure observed in these rocks indicate that these rocks were cumulates crystallized from basaltic magma infiltrating into the mantle beneath Oki-Dogo Island prior to ascent of the host magma. Hence these rocks would be formed as cumulates within magma chamber in the lower crust, and then recrystallized under subsolidus condition.

3.5. Comparison with geophysical observation

In general, Moho depth can be estimated using seismological methods. However, there is no seismic station available and the seismicity is very low in the Sea of Japan. Consequently, we cannot directly determine the depth of the Moho immediately underneath Oki-Dogo Island using present seismic methods. Nakamura et al. [26] defined the Moho discontinuity by the assumption of isostasy, with the depth data determined by seismic soundings and sea-floor topographic data. By the same method, we estimated the Moho depth under Oki-Dogo Island as 27 km. The Moho depths determined from spectroscopic and seismological methods show good agreement. The Moho depth that was estimated from the present spectroscopic method was inferred from rock samples comprising lava erupted long ago. The K–Ar age of the alkali basalts was reported as 3.30±0.12 Ma [27]. In other words, the Moho depth determined from microanalyses of CO_2 fluid inclusions indicates the depth of the crust–mantle boundary before the xenoliths were erupted to the surface. On the other hand, the Moho depth determined from the seismic technique reflects the present tectonic structure. The mantle xenoliths studied here implied much older Moho depth than the seismic technique did. The present study found that the Moho depth (27–29 km) determined by the spectroscopic method is fairly similar to the value obtained by the geophysical observation (27 km). It remains unclear whether or not this remarkable coincidence is attributable to the tectonic standstill since the eruption of xenolith (3.30±0.12 Ma).

There is an upper limit of measurable depth using the present method. Dense CO_2 fluid inclusions must be retained in silicate minerals without decrepitation. The CO_2 density of 1.2 g/cm^3 in fluid inclusions is approximately the maximum for olivine to withstand decrepitation, which occurs when the internal pressure within the fluid inclusion is greater than the strength of the host mineral [28,29]. The pressure where the CO_2 fluid inclusion with density of 1.2 g/cm^3 equilibrated with ambient condition at 1000 °C and 1300 °C is estimated to be around 1.2 GPa and 1.5 GPa, respectively (see Fig. 5), corresponding depth of around 40 km and 50 km, respectively. Pressures for garnet-bearing mantle xenoliths, which are derived from >2 GPa (~70 km), can be estimated from a garnet–orthopyroxene barometer [e.g., [30]]. Thus, there still be difficulty to study mantle xenoliths derived from 1.5–2.0 GPa.

3.6. Application to geothermal structure of lithosphere

The thermobarometric data of xenoliths enable us to understand the thermal structure of the shallow lithosphere. Applying the present temperature and pressure condition of the Moho discontinuity, the heat flow around Oki-Dogo Island is estimated to be 130–150 mW/m^2 from modeled geotherms [e.g., [1,31]]. The Sea of Japan was formed in a short period by magma eruption between the Eurasian continent and Japan arc at 11–17 Ma [32]. The plate models, GDH-1 and CHABLIS proposed by Stein and Stein [33] and Doin and Fleitout [34] respectively, representing the thermal evolution of the cooling oceanic lithosphere, indicates that the surface heat flow of the oceanic lithosphere with the age of 11–17 Ma is 120–150 mW/m^2, which is analogous to that of Oki-Dogo Island. The lower crust and the uppermost mantle under Oki-Dogo Island have not been influenced by any considerable thermal events after the opening of the Sea of Japan. This relatively "normal" heat flow for young oceanic lithosphere is absolutely an essential information for understanding the mechanism by which back arc basins are formed.

4. Conclusions

By applying micro-Raman spectroscopic analyses, we determined the densities of the CO_2 fluid inclusions in the xenoliths derived from lower crust and the uppermost

mantle sampled from Oki-Dogo Island in the Sea of Japan. The densities of CO_2 in mafic granulite and lherzolites are 1.02–1.05 g/cm^3 and 0.98–1.02 g/cm^3, respectively. Extrapolation of the densities to equilibrium temperature estimated from the two-pyroxene geothermometer indicates that the mafic granulite and lherzolites were originated from depths of 27–30 km and 25–29 km, respectively. From these overlapping values, we can therefore estimate the depth to the Moho discontinuity under Oki-Dogo Island as 27–29 km. The present spectroscopic method introduces the possibility of deciphering ancient tectonic structures from pieces of rock fragments containing CO_2 fluid inclusions.

Acknowledgements

An anonymous reviewer provided thoughtful and helpful comments to improve the manuscript. Comments from professors S. Arai and H. Iwamori are also gratefully acknowledged. We thank Mr. K. Yawata for his assistance on the field trip. We are grateful to Professors E. Takahashi, D. Zhao, K. Notsu, Drs. G.P Glasby and T. Shibata for discussion. This study was supported by a Grant-in-aid for the 21st Century COE Program for KAGI21 (Kyoto University, G3) and for Frontiers in Fundamental Chemistry and Grants-in-aid for Scientific Research (Nos. 13554018, 14654096, 15340190 and 18740344) from the Japan Society for the Promotion of Science. The manuscript was completed during HK's short-term stay at the Centre for Science at Extreme Conditions (CSEC) and the Grant Institute of Earth Sciences of the University of Edinburgh.

References

[1] X. Xu, O. Reilly, X. Zhou, W.L. Griffin, A xenolith-derived geotherm and the crust–mantle boundary at Qilin, southeastern China, Lithos 38 (1996) 41–62.
[2] T.P. Köhler, G.P. Brey, Calcium exchange between olivine and clinopyroxene calibrated as a geothermobarometer for natural peridotites from 2 to 60 kb with applications, Geochim. Cosmochim. Acta 54 (1990) 2375–2388.
[3] O. Navon, High internal pressures in diamond fluid inclusions determined by infrared absorption, Nature 353 (1991) 746–748.
[4] M. Schrauder, O. Navon, Solid carbon dioxide in a natural diamond, Nature 365 (1993) 42–44.
[5] E.S. Izraeli, W. Harris, O. Navon, Raman barometry of diamond formation, Earth Planet. Sci. Lett. 173 (1999) 351–360.
[6] H. Kagi, R. Lu, P. Davidson, A. Goncharov, H.-K. Mao, J.R. Hemley, Evidence for ice VI as an inclusion in cuboid diamonds from high P–T near infrared spectroscopy, Min. Mag. 64 (2000) 1057–1065.
[7] H. Kagi, A. Kiyasu, T. Akagi, M. Nara, T. Sawaki, Near infrared spectroscopy determines salinity and internal pressure of fluid inclusions in minerals, Appl. Spectrosc. 60 (2006) 430–436.
[8] D.A. Zedgenizov, H. Kagi, V.S. Shatsky, N.V. Sobolev, Carbonatitic melts in cuboid diamonds from Udachnaya kimberlite pipe (Yakutia): evidence from vibrational spectroscopy, Mineral. Mag. 68 (2004) 61–73.
[9] E. Roedder, Geobarometry of ultramafic xenoliths from Loihi seamount, Hawaii, on the basis of CO_2 inclusions in olivine, Earth Planet. Sci. Lett. 66 (1983) 369–519.
[10] T. Andersen, S.Y. O'Reilly, W.L. Griffin, The trapped fluid phase in upper mantle xenoliths from Victoria, Australia: implications for mantle metasomatism, Contrib. Mineral. Petrol. 88 (1984) 72–85.
[11] B. De Vivo, M.L. Frezzotti, A. Lima, R. Trigila, Spinel lherzolite nodules from Oahu Island (Hawaii): a fluid inclusion study, Bull. Mineral. 111 (1988) 307–319.
[12] J. Yamamoto, H. Kagi, I. Kaneoka, Y. Lai, V.S. Prikhod'ko, S. Arai, Fossil pressures of fluid inclusions in mantle xenoliths exhibiting rheology of mantle minerals: implications for the geobarometry of mantle minerals using micro-Raman spectroscopy, Earth Planet. Sci. Lett. 198 (2002) 511–519.
[13] Y. Kawakami, J. Yamamoto, H. Kagi, Micro-Raman densimeter for CO_2 inclusions in mantle-derived minerals, Appl. Spectrosc. 57 (2003) 1333–1339.
[14] J. Yamamoto, H. Kagi, Extended micro-Raman densimeter for CO_2 applicable to mantle-originated fluid inclusions, Chem. Lett. 35 (2006) 610–611.
[15] E. Takahashi, Finding spinel–lherzolite inclusions on Oki-Dogo Island, Japan, J. Geol. Soc. Jpn. 81 (1975) 81–83 (in Japanese with English abstract).
[16] E. Takahashi, Petrologic model of the crust and upper mantle of the Japanese island Arcs, Bull. Volcanol. 41 (1978) 529–547.
[17] E. Takahashi, Petrology of the upper mantle and lower crust of the Japanese Island arcs. Doctoral Thesis, University of Tokyo, Tokyo, Japan, 1978.
[18] N. Abe, M. Takami, S. Arai, Petrological feature of spinel lherzolite xenolith from Oki-Dogo Island: an implication for variety of the upper mantle peridotite beneath southwestern Japan, Isl. Arc 12 (2003) 219–232.
[19] K. Uto, E. Takahashi, E. Nakamura, I. Kaneoka, Geochronology of alkali volcanism in Oki-Dogo Island, southwest Japan: geochemical evolution of basalts related to the opening of the Japan Sea, Geochem. J. 28 (1994) 431–449.
[20] P.R.A. Wells, Pyroxene thermometry in simple and complex systems, Contrib. Mineral. Petrol. 62 (1977) 129–139.
[21] E. Takahashi, Origin of basaltic magmas — implications from peridotite melting experiments and an olivine fractionation model, Bull. Volcanol. Soc. Jpn. 30 (1986) 17–40.
[22] S. Fukura, T. Mizukami, S. Odake, H. Kagi, Factors determining the stability, resolution, and precision of a conventional Raman spectrometer, Appl. Spectrosc. 60 (2006) 946–950.
[23] Q. Bai, S.J. Mackwell, D.L. Kohlstedt, High-temperature creep of olivine single crystals 1. Mechanical results for buffered samples, J. Geophys. Res. 96 (1991) 2441–2463.
[24] S.J. Mackwell, High-temperature rheology of enstatite: implications for creep in the mantle, Geophys. Res. Lett. 18 (1991) 2027–2030.
[25] K.S. Pitzer, S.M. Sterner, Equations of state valid continuously from zero to extreme pressures for H_2O and CO_2, J. Chem. Phys. 101 (1994) 3111–3116.
[26] M. Nakamura, Y. Yoshida, D. Zhao, H. Katao, S. Nishimura, Three-dimensional P- and S-wave velocity structure beneath the Ryukyu arc, Tectonophysics 369 (2003) 121–143.
[27] I. Kaneoka, E. Takahashi, S. Zashu, K–Ar ages of alkali basalts from the Oki-Dogo Island, J. Geol. Soc. Jpn. 83 (1977) 187–189.

[28] T. Andersen, E.-R. Neumann, Fluid inclusions in mantle xenoliths, Lithos 55 (2001) 301–320.
[29] N. Hirano, J. Yamamoto, H. Kagi, T. Ishii, Young, olivine xenocryst-bearing alkali-basalt from the oceanward slope of the Japan, Contrib. Mineral. Petrol. 148 (2004) 47–54.
[30] K.G. Nickel, D.H. Green, Empirical geothermobarometry for garnet peridotites and implications for the nature of the lithosphere, kimberlites and diamonds, Earth Planet. Sci. Lett. 73 (1985) 158–170.
[31] J.-H. Yu, S.Y. O'Reilly, W.L. Griffin, X. Xu, M. Zhang, X. Zhou, The thermal state and composition of the lithospheric mantle beneath the Leizhou Peninsula, South China, J. Volcan. Geotherm. Res. 122 (2003) 165–189.
[32] I. Kaneoka, K. Notsu, Y. Takigami, K. Fujioka, H. Sakai, Constraints on the evolution of the Japan Sea based on ^{40}Ar–^{39}Ar ages and Sr isotopic ratios for volcanic rocks of the Yamato Seamount chain in the Japan Sea, Earth Planet. Sci. Lett. 97 (1990) 211–225.
[33] C.A. Stein, S. Stein, A model for the global variation in oceanic depth and heat flow with lithospheric age, Nature 359 (1992) 123–129.
[34] M.P. Doin, L. Fleitout, Thermal evolution of the oceanic lithosphere: an alternative view, Earth Planet. Sci. Lett. 142 (1996) 121–136.